A Geospatial Analysis of Convective Rainfall Regions Within Tropical Cyclones After Landfall

Corene J. Matyas, University of Florida, USA

ABSTRACT

In this article, the author utilizes a GIS to spatially analyze radar reflectivity returns during the 24 hours following 43 tropical cyclone (TC) landfalls. The positions of convective rainfall regions and their areal extent are then examined according to storm intensity, motion, vertical wind shear, time until extratropical transition, time after landfall, and distance from the coastline. As forward velocity increases in conjunction with an extratropical transition, these regions move outward, shift from the right side to the front of the TC, and grow in size. A similar radial shift, but with a decrease in areal extent, occurs as TCs weaken. Further quantification of the shapes of these regions could yield a more spatially accurate assessment of where TCs may produce high rainfall totals.

Keywords: *GIS, Landfall, Precipitation, Radar, Storm Motion, Tropical Cyclone, Wind Shear*

INTRODUCTION

Tropical cyclones (TCs) can produce high rainfall totals that lead to flooding both near the coastline where fast winds and storm surges are also of concern, and hundreds of kilometers away from the location of landfall (Rappaport, 2000). For example, more than 150 lives were lost from fresh water flooding as Hurricane Camille (1969) produced record rainfall totals nearing 700 mm in Virginia. Several days earlier, most deaths that occurred during the landfall of Hurricane Camille resulted from the high storm surge (Schwarz, 1970). Recently, the original rainfall climatology and persistence (R-CLIPER) statistical model developed to verify rainfall predictions for TCs (Marchok, Rogers, & Tuleya, 2007) has been upgraded to include the effects of vertical wind shear and topography as these characteristics have been shown to cause asymmetries in TC rain fields (Lonfat, Rogers, Marchok, & Marks, 2007). However, as recently as 2007, the American Meteorological Society stated that rainfall predictions for landfalling TCs are still in need of improvement (AMS, 2007).

DOI: 10.4018/jagr.2010020905

Although stratiform clouds can cover ten times more area within a TC than convective clouds (Jorgensen, 1984), the higher rainfall rates produced by convective clouds can produce flooding rainfall in a relatively short amount of time (Geerts et al., 2000; Elsberry, 2002). Even though Hurricane Floyd (1999) was moving at a relatively fast forward velocity of 9 m s^{-1} during landfall, the high rain rates produced by convective processes caused more than 500 mm of rain to accumulate (Lawrence et al., 2001; Atallah & Bosart, 2003). Thus, identifying the conditions under which convective clouds cover a large area within a TC's rain fields, and where these areas of convection will exist relative to the circulation center of a TC is an important task.

This study employs geospatial research techniques to examine convective rainfall regions that exist during the 24-hour period after TCs make landfall. Specifically, three research goals are pursued: 1) determine where regions of heavy rainfall exist in relation to the circulation center of the TC under different conditions, 2) determine the areal extent, or size, of these rainfall regions, and 3) determine the conditions under which the largest areas of heavy rainfall tend to form. To achieve these research goals, radar reflectivity returns are analyzed within a GIS to locate the heavy rainfall regions and to calculate the spatial properties of these regions as they relate to six factors. These factors are a) storm intensity, b) vertical wind shear, c) storm motion, d) whether or not a TC becomes extratropical, e) the time elapsed after landfall, and f) the distance that the storm and its convection are located relative to the coastline. In addition to achieving these research goals, this study analyzes a large number of TCs in a GIS framework.

BACKGROUND

Willoughby, Marks, and Feinberg (1984) describe the regions of convection that develop in both the core of a hurricane (within 100 km of the circulation center), and in the outer rainbands that can extend more than 360 km from the circulation center of the storm. Convection is enhanced by increased surface friction along the coastline during landfall (Tuleya, 1994; Frank & Ritchie, 1999), and fast tangential winds can advect moisture counterclockwise into the left front quadrant in the core of a hurricane (Parrish, Burpee, Marks, & Grebe, 1982). Konrad, Meaux, and Meaux (2002) found that intense TCs have increased rainfall near the core of the storm. On the other hand, tropical depressions have very little organized convection in their core (Frank & Ritchie, 1999). These findings suggest that storm intensity could exhibit a strong relationship with both the location of convection relative to the circulation center of the storm and the size of the area covered by convective rainfall.

A recent modeling study by Kimball (2008) found that rainfall spreads outwards from the circulation center as a TC tracks inland, and shifts from a maximum on the right side of the storm to the front of the storm in a counterclockwise direction. Observational studies of individual TCs have demonstrated that convection within TCs may increase or decrease in spatial extent after landfall (e.g., Bluestein & Hazen, 1989; Atallah & Bosart, 2003; Medlin, Kimball, & Blackwell, 2007; Matyas, 2008). Time elapsed after landfall may demonstrate an association with these trends in the location and areal extent of TC convection. However, the influence of the atmosphere, internal storm dynamics, and the earth's surface may exhibit an even stronger association with the position and size of convective regions during the post-landfall period. TCs that remain near to the coastline after landfall may be able to advect moisture into their circulation so that rainfall does not diminish as quickly as it would if the storm had moved directly inland (Medlin et al., 2007). Thus, the location of the TC or its convection relative to the coastline could be related to the position and/or the areal extent of convection.

Several observational studies have shown that vertical wind shear causes an asymmetrical distribution of rainfall about the center of a TC so that the majority of rainfall occurs in

the downshear direction (Molinari, Moore, & Idone, 1999; Corbosiero & Molinari, 2002; Cecil, 2007). Other studies have focused on the asymmetries in the rain fields of TCs produced by storm motion (e.g., Burpee & Black, 1989; Rodgers, Baik, & Pierce, 1994; Lonfat, Marks, & Chen, 2004), finding that rainfall shifts to a location ahead of the storm as forward velocity increases. When Corbosiero and Molinari (2003) and Chen, Knaff, and Marks (2006) examined the contributions of both storm motion and vertical wind shear to the distribution of TC rainfall, they determined that vertical wind shear exerts the dominant influence, while storm motion controls rainfall distribution only when vertical wind shear is weak. However, these authors only examine lightning flashes and areas of rainfall within 300 and 330 km of the storm centers, respectively, whereas research by Lonfat et al. (2004) show that convective rainfall can occur 500 km from the circulation center of a TC.

When TCs become extratropical, they experience both strong vertical wind shear and an increase in forward velocity (Atallah & Bosart, 2003; Jones et al., 2003), so it stands to reason that the time until a TC becomes extratropical should exhibit a relationship to the distribution of rainfall about the circulation center of the storm in a pattern similar to that imposed by shear and storm motion. TCs that transition into extratropical systems tend to have well-developed rain fields on the left side of their storm track (Atallah & Bosart, 2003; Matyas, 2008) as rainfall expands ahead of the circulation center. For TCs that do not experience the rainfall-enhancing dynamics that occur during an extratropical transition, convective rainfall may decrease as the storm moves inland, and is removed from its source of latent energy (Tuleya, 1994; Kimball, 2008), and is surrounded by drier continental air masses (Cubukcu, Pfeffer, & Dietrich, 2000; Hill & Lackmann, 2009).

DATA

Radar reflectivity returns from multiple Weather Surveillance Radar-1988 Doppler (WSR-88D) sites are utilized to determine where heavy rainfall is located relative to the TC's center of circulation. These data are obtained from the National Climatic Data Center's NEXRAD data archive (http://www.ncdc.noaa.gov/nexrad-inv/). Base reflectivity data from the Level III WSR-88D products are utilized whenever available. In cases where only the raw Level II data are available, data from the lowest scan elevation are utilized for the spatial analysis. Additional information pertaining to Level II and III radar data are available in the Federal Meteorological Handbook 11-Part C (Office of the Federal Coordinator for Meteorology, 2006).

Archives for many of the 159 WSR-88D sites extend from 1995 through the present, allowing landfalling TCs during 1995-2008 to be examined in the current study. Due to problems with the archiving system at the National Climatic Data Center, data for several TCs are not available at the time of this study, including all TCs from the 1998 season. For a TC to be analyzed in the current study, its rain fields must be within range of the WSR-88D network for a 24-hour period following the time of landfall. Thus, TCs that either dissipate within 24 hours of landfall (e.g., Matthew (2004)), or that did not remain over land for 24 consecutive hours after landfall (e.g., Charley (2004), Wilma (2005)) are not included in the study. As a second U.S. landfall occurs for some TCs more than 24 hours after the first landfall, these subsequent landfalls are also analyzed. Overall, this study examines 43 U.S. landfalls from 38 TCs.

Data pertaining to the latitude and longitude of the circulation centers of the TCs are obtained from two sources. The position of the circulation center at the time of landfall is taken from the National Hurricane Center (NHC)'s Hurricane Season Tropical Cyclone Report for each storm (http://www.nhc.noaa.gov/pastall.shtml). These reports also provide the date and time of landfall. For this study, the time of landfall is rounded to

the nearest half-hour. The position of the storm at all other analysis times, as well as its intensity as measured by the maximum sustained wind speed, forward velocity and heading and stage of the storm, are obtained from the Hurricane Database (HURDAT) maintained by the NHC (2006). This database contains observations for all TCs in the North Atlantic Ocean basin every six hours at 0000, 0600, 1200, and 1800 UTC. A linear interpolation is performed to obtain data in three-hourly time steps beginning at the time of landfall and ending 24 hours later. This process yields nine observation times for each TC landfall, or 387 total observation times for the 43 landfalls examined. The number of hours until a TC becomes extratropical is also calculated at each observation time for TCs that became extratropical either during the study period or up to 72 hours after landfall.

The velocity and direction of the vertical wind shear are acquired from the Statistical Hurricane Intensity Scheme (SHIPS) database (DeMaria & Kaplan, 1994; DeMaria, Mainelli, Shay, Knaff, & Kaplan, 2005). SHIPS data are available for TCs in both the Atlantic and eastern Pacific Ocean basins at 0000, 0600, 1200, and 1800. The vertical wind shear is the difference betweeen the 200 and 850 hPa winds calculated for an annular region located 200-800 km from the circulation center of each TC. The SHIPS data are also interpolated linearly to obtain data in three-hourly time steps beginning at the time of landfall and ending 24 hours later.

ANALYSIS

To identify regions of heavy rainfall within the rain fields of a TC and to calculate their spatial attributes, the radar reflectivity data are converted into a georeferenced format and imported into a GIS. Working with each three-hourly observation separately, the data from adjoining WSR-88D stations are first combined into a single raster layer with a grid size of one square kilometer. A small amount of error is introduced into the analysis due to differences in calibration among the different radars and the range-dependent beam geometry and elevation (Anagnostou, 2004). At locations where reflectivity values are available from multiple WSR-88D sites, the highest reflectivity value is retained. Figure 1 demonstrates the combining of the radar reflectivity from multiple WSR-88D sites within the GIS. Next, an interpolation is performed using inverse distance weighting to create contour lines that connect areas having the same reflectivity value. As the level III reflectivity data are available in 5 dB*Z* increments, the contour lines are also placed in 5 dB*Z* increments. The polylines created by the interpolation are then converted into polygons, and spatial attributes are calculated for each polygon, including area and the latitude and longitude of the centroid, or center of mass.

As this study is concerned with identifying regions of heavy rainfall that may have the potential to produce flooding, polygons larger than 500 km^2 in area that enclose reflectivity values of 40 dBZ or greater are retained for further analysis. As shown in Figure 2, multiple convective regions of 40 dB*Z* reflectivity values over 500 km^2 in area may exist for a TC at a given observation time, and all such areas are analyzed in the current study. TC researchers such as Jorgensen (1984) have used 40 dB*Z* reflectivity values to denote heavy rainfall within convective rainbands. Reflectivity values of 40 dB*Z* may produce rainfall rates of approximately 21.6 mm hr^{-1} (0.85 in hr^{-1}) according to the reflectivity to rain-rate conversion developed by Rosenfeld, Wolff, and Atlas (1993) for tropical systems.

This study seeks to determine which of six factors are most closely associated with the position of the convective regions relative to the circulation center of the storm, and the areal extent of these regions. These factors are the intensity of the storm as measured by the maximum sustained wind speed, the speed of the vertical wind shear and storm forward motion, whether the TC becomes extratropical, time that has elapsed since landfall, and the position of the TC and its rainfall regions relative to the coastline. Therefore, the attribute table of each convective polygon is expanded to include ad-

Figure 1. Radar reflectivity values for Hurricane Ivan (2004) at the time of landfall; The highlighted polygons represent regions having reflectivity values greater than or equal to 40 dBZ that are greater than 500 km² in areal extent

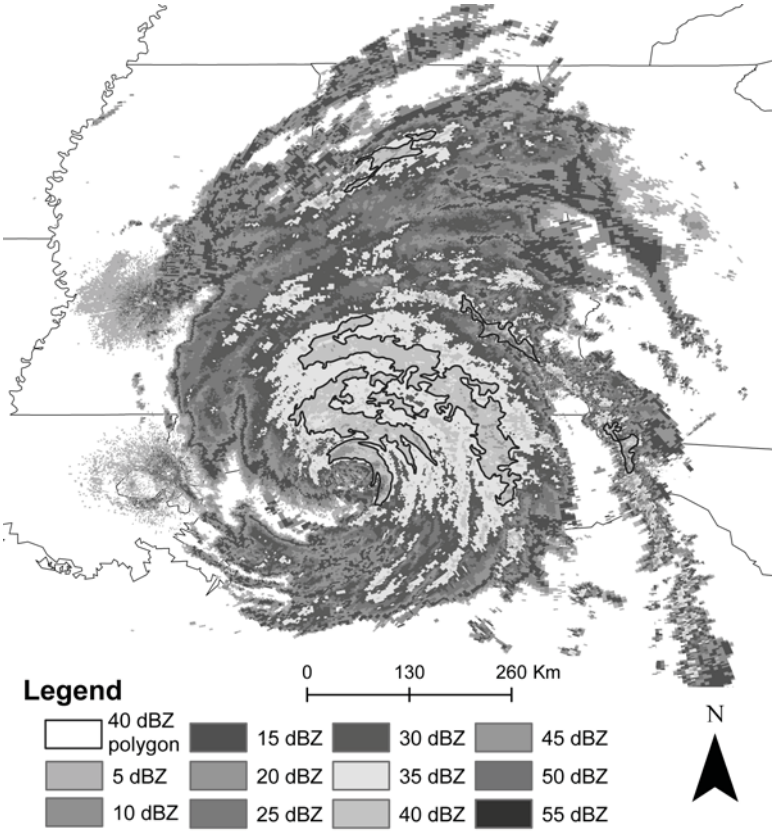

ditional information for its observation time. Columns added to the attribute table include the storm name, year, month, day, observation time, circulation center latitude and longitude, maximum sustained wind speed, direction and speed of vertical wind shear and storm motion, the number of hours since landfall, and the number of hours until the storm becomes extratropical, if applicable. The distance and bearing of each polygon centroid relative to the circulation center of the TC at each observation time is then calculated using spherical trigonometry.

The next step in the analysis is to recalculate the positions of the polygon centroids so that their bearings are in coordinates that are relative to the heading of the storm. First, the heading of the storm is subtracted from the bearing of the centroid. Next, 360° is added to negative values. Thus, polygon centroids located at bearings 0-90° are in the right-front quadrant, and centroids with bearings of 90-180°, 180-270°, and 270-360° are located in the right rear, left rear, and left front quadrants respectively. A similar process is performed to determine the shear-relative quadrants. For this calculation, the heading of the vertical wind shear is subtracted from the bearing of the centroid, and 360° is added to negative values. Polygon centroids with bearings of 0-90° are located in the downshear right quadrant, while 90-180°, 180-270°, and 270-360° are located upshear right, upshear

Figure 2. Position and intensity of Ivan (2004) and the 40 dBZ polygons that are analyzed at each 3-hourly observation time

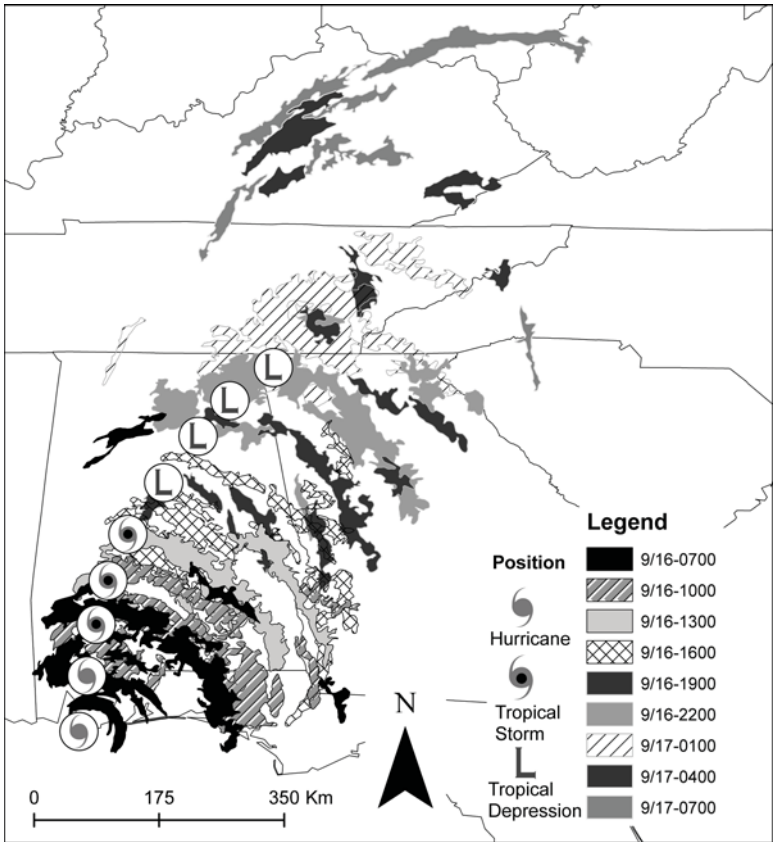

left, and downshear left respectively. The GIS is also utilized to determine the distance from each polygon centroid to the nearest point on the U.S. coastline. In all, 21 columns of data exist for each convective region.

Two strategies are employed to determine which of the six factors has the strongest association with the radial position of the convective regions relative to the circulation center of the TC. First, correlation coefficients are calculated between the distance of the convective region relative to the circulation center of the TC and the variables representing the six factors. As the data are not normally distributed, they are ranked from highest to lowest values and Spearman rank correlation coefficients (Wilks, 1995) are calculated.

The second strategy to explore patterns in the location of convection under the six factors involves grouping the convective regions according to sub-classifications of each condition. Observations are grouped by the intensity of the storm as determined by the velocity of the maximum sustained winds: 1) greater than 33 m s^{-1} for hurricanes, 2) 17-33 m s^{-1} for tropical storms, or 3) less than 17 m s^{-1} for tropical depressions. The convective regions are placed into one of three groups based on the speed of the vertical wind shear: 1) less than 5 m s^{-1}, 2) 5-10 m s^{-1}, or 3) greater than 10 m s^{-1}. This breakdown of slow, medium, and fast vertical wind shear is utilized to render the results comparable to those of Corbosiero and Molinari (2002). These same divisions are used to

group the convective regions according to the forward velocity of the TC. Four categories are developed to examine convection relative to the time that a TC becomes extratropical: 1) less than 24 hours, 2) 24-48 hours, 3) 48-72 hours, or 4) observations from TCs that did not become extratropical within 72 hours of landfall. The number of hours after landfall (0, 3, 6, 9, 12, 15, 18, 21, and 24) is also used to group the observations. Distance relative to the coastline is the final factor by which the convective regions are divided into three categories: 1) more than 25 km offshore, 2) within 25 km of the coastline either on or offshore, or 3) more than 25 km inland. These distances represent natural breaks in the data. To examine the radial positions of the convective regions, the percent of observations in 100 km-wide annular rings extending outward from the circulation center is calculated for each condition-group. The distances of convective regions that are greater than 500 km are combined. To characterize the azimuthal distribution of convection for each of the condition-groups, the percent of observations occurring in each quadrant of the storm is calculated. All quadrants are placed relative to storm motion save for the examination of data according to vertical wind shear; for this condition, quadrants are placed according to the direction of the shear vector.

To determine which of the six factors is most strongly associated with large areas of convection, a second dataset is constructed so that each observation time has only one entry. For each observation time, the areas of all 40 dB*Z* polygons over 500 km^2 in size are summed. Variables representing each factor are then added for each entry. For this dataset, the distance from the coastline variable represents the distance of the circulation center of each TC from the nearest point on the coastline as calculated within the GIS. Spearman rank correlation coefficients are then calculated to determine if the largest areal extent of convection corresponds to the largest or smallest values of the six factors. The observations are then placed into the same sub-groups for each condition as those described for the centroid distance comparisons save for the distance to the coastline. For this condition, observations are placed into one of four groups: 1) within 50 km, 2) 50-100 km, 3) 100-200 km, or 4) greater than 200 km from the coastline. For each condition-group, the average area covered by convection is calculated to determine which variables are associated with the largest area covered by convection, which might indicate the largest potential for flooding to occur.

RESULTS AND DISCUSSION

The 43 TC landfalls examined in this study have 1545 regions of convection larger than 500 km^2 during the 387 observation times (Figure 3). On average, four convective polygons are present at each observation time, but 36 observation times contain no areas of convection larger than 500 km^2. Of the 43 landfalls examined, 25 occurred when the TC was a tropical storm rather than a hurricane. By twelve hours post-landfall, only Danny (1997) and Frances (2004) remained hurricanes, and most TCs were at tropical storm intensity. Therefore, the majority of convective polygons examined in the study occur when the TC is at tropical storm intensity. Also, in nearly half of the landfalls examined, TCs became extratropical within 72 hours of landfall.

The discussion of each factor is presented in order according to the strength of its association with the location and areal extent of convection. As storm motion exhibits the strongest relationship to both the location and areal extent of convection, this factor is discussed first in both subsections. For the location of convection relative to storm center subsection, the factors are ordered as follows: forward velocity, time until extratropical transition, vertical wind shear, intensity, time after landfall, and distance to coastline. In the areal extent of convection subsection, the factors are presented as follows: forward velocity, time until extratropical transition, intensity, distance from the coastline, vertical wind shear, and time after landfall.

Figure 3. Positions of the circulation centers of the 43 TC landfalls examined in the current study categorized by intensity, and the location of the centroid of areas of convection larger than 500 km²

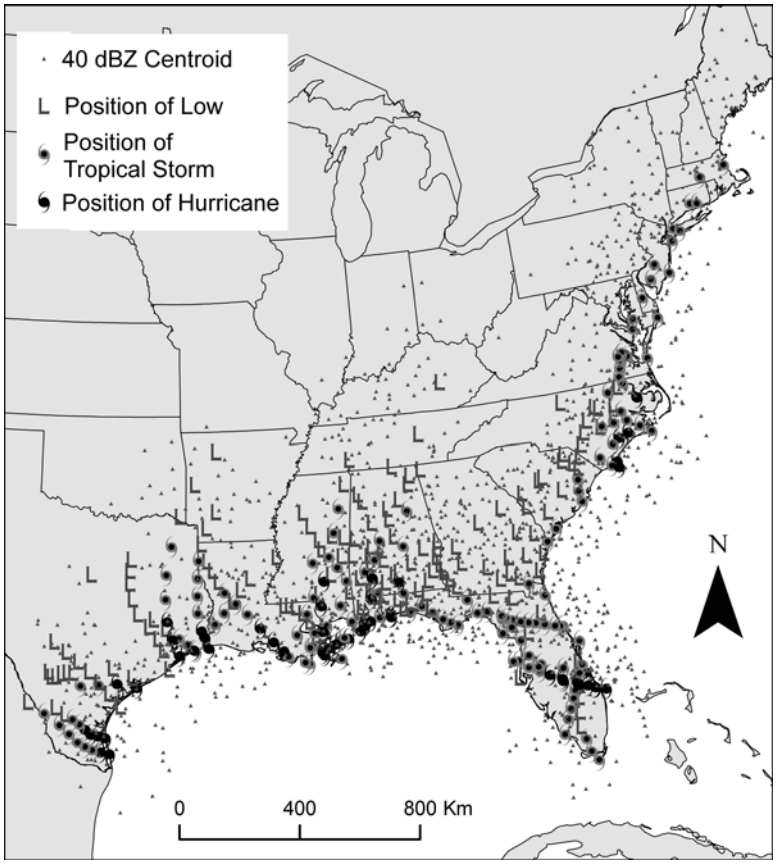

Location of Convection Relative to Storm Center

Results suggest that the forward velocity of the TC has the largest effect on the location of convection both in the azimuthal and radial directions during the 24 hours after landfall. Overall, more convection occurs on the right side of the storm rather than the left (Figure 4a), which agrees with the findings of previous research (Frank & Ritchie, 1999; Corbosiero & Molinari, 2003; Lonfat et al., 2004; Chen et al., 2006). Shapiro (1983) explains that storm motion induces asymmetries in the boundary layer frictional drag due to the stronger winds on the right side of the vortex that result when translation speed is added to the rotational speed of the tangential winds. The current study finds that in TCs moving at velocities under 5 m s^{-1}, convection is evenly split between the right front and rear quadrants of the storm. When TCs are moving at 5-10 m s^{-1}, 60% of convective observations occur in the right front quadrant and only 21% are located in the rear of the storm. Almost 55% of convective observations for TCs with forward velocities exceeding 10 m s^{-1} occur in the left front quadrant, and 95% occur in the forward half of the storm, indicating a counterclockwise shift in the location of convection as forward velocity increases. This

Figure 4. Locations of polygon centroids relative to the circulation center of the storm based on a) storm motion, b) time until becoming extratropical, c) vertical wind shear, d) intensity, e) hours since landfall, and f) location relative to the coastline. All figures save c are oriented towards the direction of storm motion with the right front quadrant at the top right of the figure. Panel c is oriented in the direction of the vertical wind shear so that downshear right is at the top right of the figure. Only centroids for convective regions in TCs that became extratropical are depicted in panel b. Annular rings are shown every 100 km out to 800 km.

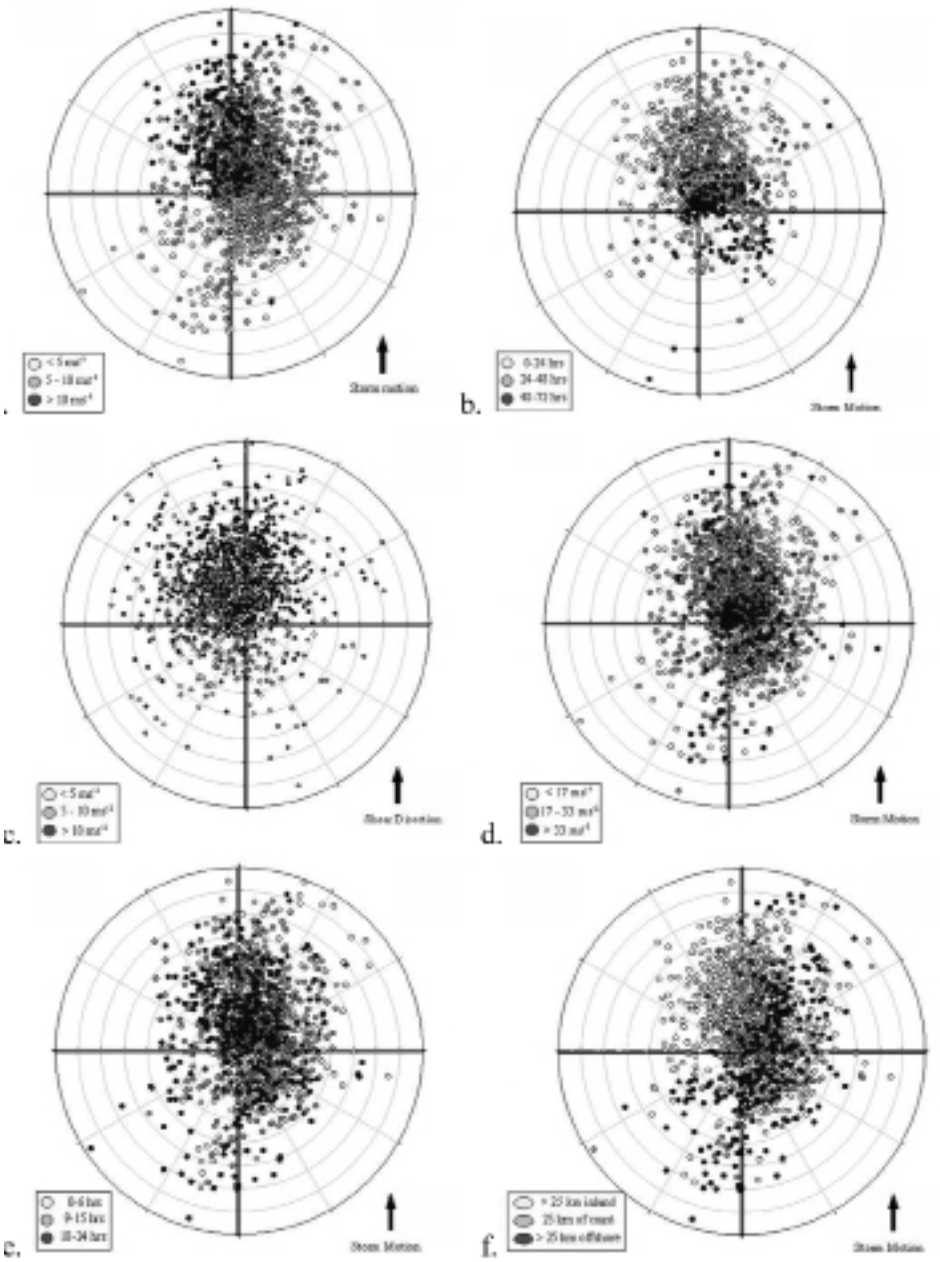

Table 1. Spearman Rank correlation coefficients for each convective region's centroid distance, and for the total areal extent of all convective regions at each observation time; Bold values are statistically significant at $\alpha = 0.01$

	Centroid Distance (n=1545)[a,b]	**Total Areal Extent (n=387)[c]**
Motion	**0.235**	**0.524**
Intensity	**-0.143**	**0.461**
Time until Extratropical	**-0.189[a]**	**0.274**
Hour since Landfall	**0.180**	**-0.252**
Shear	-0.057[b]	-0.018[c]
Distance to Coastline	0.034	0.013

[a] n = 908
[b] n = 1152
[c] n = 273

is similar to the pattern described by Kimball (2008).

Forward velocity is also important when considering the distance from the circulation center at which convection tends to occur. The correlation between centroid distance and storm forward velocity demonstrates that storm motion has the strongest association with the radial distribution of convection out of all six factors tested (Table 1). TCs moving at a fast forward velocity have 17% of convective observations located more than 500 km from the circulation center, which is the highest percentage of all other sub-groups of factors examined (Table 2). The distribution of convection is fairly similar among TCs with forward velocities below 5 m s^{-1} and 5-10 m s^{-1}. For these storms, approximately 70-75% of observations occur within 300 km of the circulation center. However, 52% of observations in TCs moving at speeds greater than 10 m s^{-1} occur beyond 300 km. This has important implications for the findings of previous research as studies examining convection only within 400 km of the circulation center (e.g., Chen et al., 2006; Cecil, 2007) may have missed as much as one third of the convection associated with fast-moving TCs. Even more importantly, studies examining data within only 300 km of the circulation center (e.g., Molinari et al., 1999; Corbosiero & Molinari, 2002; Corbosiero & Molinari, 2003) may have missed more than half of the convection that exists in fast-moving TCs.

The number of hours until a TC becomes extratropical also exhibits an association with the location of convection in TCs after landfall (Figure 4b). When a TC is within 48 hours of becoming extratropical, convection decreases markedly in the inner 100 km, while 24 hours earlier, this innermost region contains the highest percentage of observations (Table 2). In the outer region of the storm beyond 300 km, the number of convective polygons increases from 14% to 43% of the total number of observations during the same time period (Table 2). These results suggest that a spreading out of convection occurs as a storm becomes extratropical. The negative correlation between centroid distance and hours until the TC becomes extratropical (Table 1) supports this finding.

Although the majority of the convective polygons remain in the right front quadrant regardless of when or if an extratropical transition happens, a shift in the counterclockwise direction towards the left front quadrant occurs as TCs approach the time that they become extratropical

Table 2. Percent of polygon centroids representing convective regions contained within each 100 km annulus outward from the storm center, and the total number of centroids per condition-group. Bold values indicate the distances with the highest percentage of observations.

Analysis	n	0-100km	100-200km	200-300km	300-400km	400-500km	500+ km
Motion							
< 5 ms^{-1}	566	21	**33**	24	14	5	3
5-10 ms^{-1}	736	17	**29**	23	16	8	8
> 10 ms^{-1}	234	12	16	**21**	20	15	17
Time until Extratropical							
0 - 24 hrs	466	12	**23**	**23**	**23**	12	9
24 - 48 hrs	297	13	26	**27**	16	7	11
48 - 72 hrs	145	**34**	28	23	10	1	3
None	527	22	**34**	21	12	6	6
Shear							
< 5 ms^{-1}	132	18	**33**	23	12	8	6
5-10 ms^{-1}	306	16	**31**	29	12	7	6
> 10 ms^{-1}	714	21	**31**	21	14	6	7
Intensity							
Hurricane	288	**28**	26	20	8	8	9
Trop. Storm	870	17	**31**	23	16	6	7
Trop. Dep.	387	10	24	**25**	21	12	8
Hours since Landfall							
0	200	24	**32**	26	9	4	7
3	203	27	**32**	16	12	5	8
6	193	21	**34**	20	12	5	8
9	200	17	24	**26**	20	8	5
12	180	17	26	**27**	17	8	5
15	161	11	**26**	22	21	14	6
18	157	12	**29**	20	12	15	11
21	134	12	26	**28**	19	4	10
24	117	11	21	24	**26**	9	9
Coastline Proximity							
Offshore	299	7	**28**	26	17	10	12
Near Coast	291	24	**27**	22	15	7	4
Inland	933	19	**29**	23	16	7	6

(Figure 4b). At 48-72 hours before becoming extratropical, nearly 50 (25) % of convection is in the right front (rear) quadrant. Twenty-four hours later, the right front (rear) quadrant contains 61 (10) % of the convection, while the percentage of observations within left front quadrant increases only slightly. However, in the next 24 hours, the amount of convection in the right (left) front quadrant decreases (increases) to 49 (42) %, completing the counterclockwise shift. Ritchie and Elsberry (2001) and Atallah and Bosart (2003) explain that this shift in the azimuthal location of convection occurs when relatively cool and dry air that diminishes convection advects counterclockwise around the circulation center beginning southwest of the TC. Meanwhile, convective precipitation is enhanced to the north of the circulation center as the warm and moist air of tropical origin on the eastern side of the TC is uplifted.

The speed of the vertical wind shear appears to exert a stronger influence on the azimuthal rather than the radial distribution of convection after landfall (Figure 4c). When all observations are considered, most of the convection is located in the downshear left and right quadrants, which is in agreement with the findings of Corbosiero and Molinari (2002), Chen et al. (2006), and Cecil (2007). However, a clockwise shift in the position of the convective regions is observed as vertical wind shear increases. For TCs experiencing vertical wind shear speeds less than 5 m s^{-1}, 39 (28)% of the observations occur in the downshear (upshear) left quadrant. When the velocity of the vertical wind shear increases to 5-10 m s^{-1}, the number of observations increases (decreases) to 53 (17) % in the downshear (upshear) left quadrant. When strong vertical wind shear is present, only 6% of observations are located in both upshear quadrants, while 53 (36) % are located in the downshear left (right) quadrants. This clockwise shift in convection with increasing vertical wind shear has not been discussed by previous researchers. Figures from Corbosiero and Molinari's (2002) study only indicate that the downshear quadrants experience the most lightning flashes in both the inner 100 km and outer 100-300 km regions of the storm regardless of the strength of the vertical wind shear.

While the speed of the vertical wind shear appears to influence the azimuthal distribution of convection, it has a much weaker association with the radial distribution of convection as compared to storm motion. Approximately 30% of convective observations are located 100-200 km from the circulation center, and less than 20% are located in either the inner core, or beyond 400 km regardless of the velocity of the vertical wind shear. This suggests that stronger wind shear values do not result in the development or displacement of convection farther from the circulation center. The lack of a statistically significant correlation between the velocity of the vertical wind shear and the distance of the convective observations relative to the storm center (Table 1) supports this finding.

Convection is present in both the core and outer rainbands of hurricanes, while weaker TCs have little convection present within their core (Table 2). Hurricanes have nearly the same number of convective regions within 100 km of the circulation center, which includes convection found in the eyewall, as they do in the region 100-200 km from the circulation center (Table 2), where the edge of the principal rainband is often located (Willoughby et al., 1984; Molinari et al., 1999). Tropical storms have a clear maximum in convection 100-200 km from the circulation center. Tropical storms have more convection in the storm core than do tropical depressions, but much less convection near the core of the storm than do hurricanes (Table 2). Twice as many convective observations are located 300-400 km from the circulation centers of tropical depressions than within the innermost 100 km, indicating a lack of convection near the core of tropical depressions (Table 2). The negative correlation coefficient between intensity and the distance of the observations from the circulation center indicates that higher intensity correlates to a closer centroid distance (Table 1). This result suggests that convection spreads outwards as the TCs weaken. As the majority of the observations occur on the right side of the storm (Figure 4d) in all three sub-

groups, intensity does not appear have as strong of an association with the quadrant in which convection is located as does storm motion and vertical wind shear.

When the locations of convection are examined based upon the time that has elapsed since landfall, the spreading out of convection with time that is discussed by Kimball (2008) is evident. However, the outward spread of convection does not appear to happen steadily over time. The radial distribution of convective polygons is similar during the first six hours post-landfall, when approximately 55% are located within 200 km of the circulation center and only 12% are located beyond 400 km (Table 2). From 9 to 12 hours post-landfall, convection diminishes in storm core, but remains the same in the region beyond 400 km. Over the next 6 hours, the percentage of observations located over 400 km away from the storm center doubles. Towards the end of the 24-hour period, the amount of convection in the farthest distances diminishes, but the distance of most convective observations shifts outwards from 200-300 km to 300-400 km.

A counterclockwise shift in the location of convection is not observed when time after landfall is the only variable considered (Figure 4e). The number of convective regions in each motion-relative quadrant remains fairly consistent for the first 21 hours post-landfall. The percent of observations occurring in the right front, right rear, left rear, and left front quadrants are approximately 50%, 20%, 10%, and 20% respectively. However, at 24 hours post-landfall, the maximum shifts to the right rear quadrant, with 32% of the observations. Most of these observations belong to slow-moving tropical depressions, and slow-moving TCs tend to have more convection present in the right rear quadrant of the storm than in the left front quadrant, possibly due to the advection of moisture from the ocean (Bluestein & Hazen, 1989). Analysis of additional hours post-landfall is required to determine if a maximum in the left front quadrant emerges at a later time.

The distance at which convection forms relative to the coastline appears to have some association with the azimuthal distribution of convection relative to the circulation center of the storm. Figure 4a shows that convection exists in the left rear quadrants of some TCs despite this area being the most unfavorable location for the formation of convection given that downward vertical motion is enhanced on the left side of a TC (Powell, 1990). While many TCs track inland after landfall, some travel across the peninsula of Florida (e.g., Jeanne (2004) and Erin (1995)) or track parallel to the U.S. coastline (Floyd (1999) and Hanna (2008)). Thus, convection located more than 25 km offshore may occur in any motion-relative quadrant of the storm. In this study, over 50% of the offshore convection is located in the rear quadrants of the TCs (Figure 4f). The 45% of offshore observations located in the right front quadrant are associated with TCs making landfall along the east coast of the U.S. and moving towards the north, for example Floyd (1999) and Hanna (2008). Offshore observations located the farthest from the circulation center in the right front quadrant exist in TCs that are nearing the time at which they become extratropical.

Results from the analysis of the near-shore observations suggest that the coastline does exert an influence on the azimuthal location of convection as TCs make landfall and move inland. Previous studies have discussed how frictional convergence produced along the coastline along the right side of the storm enhances the development of convection as a TC makes landfall (e.g., Jones, 1987; Frank & Ritchie, 1999). However, more than 35% of the observations occur in the two rear quadrants of the storm, suggesting that the coastline influences convective precipitation even after the circulation center has moved inland. Additionally, since convection occurs near the coastline more than 300 km away from the circulation center, coastal areas not affected by the strongest winds in a landfalling TC may still experience heavy precipitation.

Areal Extent of Convection

The largest regions of convection are associated with fast-moving TCs that are nearing the time of transition to extratropical and located within 50 km of the coastline. Of these three factors, storm motion has the strongest relationship with the areal coverage of convection (Table 1). TCs that are moving at speeds exceeding 10 m s^{-1} have larger areas covered by convection on average than any of the other sub-groups examined (Table 3). The nearly 30,000 km^2 average areal coverage of convection for fast-moving TCs is 20,000 km^2 more than for TCs moving at 5-10 m s^{-1}, and approximately 10,000 km^2 more than for TCs that are within 24 hours of becoming extratropical. The top ten largest convective areas occur in TCs with forward velocities greater than 8 m s^{-1}, and very few TCs that are moving at this speed have small areas of convection (Figure 5a).

Interaction with a middle latitude trough is what typically causes storm motion to increase, and is also what causes the TC to become extratropical (Jones et al., 2003). All of the observation times that feature TCs moving at speeds greater than 10 m s^{-1} also occur when TCs are within 24 hours of becoming extratropical. However, all TCs within 24 hours of becoming extratropical do not necessarily move at fast forward velocities. Nearly 60% of the observations from this group occur when forward velocity is below 10 m s^{-1}. As a TC becomes extratropical, the surrounding environment becomes baroclinic and the isentropic ascent of the moist air mass associated with the TC enhances precipitation and causes the region within which heavy rainfall occurs to increase in area (Atallah & Bosart, 2003; Jones et al., 2003). As a group, TCs that are within 24 hours of being extratropical have the second largest areas of convection on average (Table 3). The ten largest areas of convection are associated with Floyd (1999), Hanna (2008), and Bertha (1996), which moved towards the north parallel to the east coast of the U.S. (Figure 3) at speeds greater than 9 m s^{-1} as they transitioned into extratropical storms. The average area of convection increases for TCs as the time until their extratropical transition (Table 3). The statistically significant correlation coefficient between total areal extent of convection and time until becoming extratropical (Table 1) also supports the finding that extratropical transition results in larger regions of convection. For TCs that do not experience an extratropical transition, convection develops over an area of approximately 22,000 km^2 in the largest case (Figure 5b), but convection is more commonly confined to an area measuring approximately 5000 km^2 (Table 3).

The second largest correlation with convective area is the maximum sustained wind speed (Table 1), indicating that the area covered by convection is largest for hurricanes and decreases as TCs weaken. Although the five largest regions of convection belong to tropical storms (Figure 5c), numerous regions smaller than 1000 km^2 exist for both tropical storms and tropical depressions. In hurricanes, however, the smallest region is more than 2100 km^2 in size. Hurricanes have convection in both their core and in their outer rainbands so that greater total area is covered by convective rainfall than for weaker TCs. This finding is consistent with that of Shepherd et al. (2007). Also contributing to the large spatial coverage of convection for hurricanes is their location close to the coastline. When the TC is located inland and the tangential winds are weaker, it is more difficult to advect moisture from the ocean into the circulation to sustain heavy rainfall (Bluestein & Hazen, 1989). The exception to the trend of diminishing convection as maximum sustained winds weaken after landfall occurs when TCs become extratropical. Many of these TCs are at tropical storm intensity as the size of their convective area grows.

As a group, TCs located within 50 km of the coastline have the third largest areal extent of convection out of the 26 sub-groups examined (Table 3). Once a TC is more than 100 km inland, no areas of convection larger than 25,000 km^2 are present (Figure 4d). This is likely because less moisture is available over the land surface for latent heat flux (Tuleya, 1994; Kimball,

2008), and continental air masses surrounding the TC have less available moisture to enhance rainfall (Bluestein & Hazen, 1989; Cubukcu et al., 2000). As previously discussed, many

Table 3. The average areal extent of convection for each condition-group and the number of observations contained within each condition-group; Bold values indicate group with the largest areal coverage of convection for each condition

Analysis	n	Average Area (km^2)
Motion		
< 5 ms^{-1}	175	5842
5-10 ms^{-1}	149	10340
> 10 ms^{-1}	32	**29975**
Time until Extratropical		
0 - 24 hrs	87	**18994**
24 - 48 hrs	51	13407
48 - 72 hrs	33	6307
none	176	5253
Intensity		
Hurricane	56	**13039**
Trop. Storm	178	11676
Trop. Dep.	121	5849
Coastline Proximity		
< 50 km	149	**14773**
50-100 km	67	6989
100-200 km	69	5787
> 200 km	65	6281
Shear		
< 5 ms^{-1}	45	4568
5-10 ms^{-1}	110	4781
> 10 ms^{-1}	118	**12273**
Hours since Landfall		
0	43	9056
3	43	9140
6	43	10248
9	43	9973
12	40	**11611**
15	38	10816
18	37	11119
21	33	10676
24	34	6356

of the TCs that remain within 100 km of the coastline several hours post-landfall experience an extratropical transition that helps to increase the area over which convective rainfall occurs. Despite the clear tendency for inland TCs to have smaller convective rainfall regions, a statistically significant correlation does not exist between a TC's distance from the coastline and the area of its convection (Table 1). When TCs are close to the coastline, areas of strong convection present in the eyewalls of hurricanes as well as convection enhanced by friction along the coastline in the outer rainbands have a limited spatial extent, which accounts for many of the regions of convection that occupy less than 10,000 km^2 visible in Figure 5d.

TCs experiencing vertical wind shear velocities above 10 m s^{-1} have a larger area of

Figure 5. The total area covered by convection at each observation time compared to: (a) storm motion, (b) time until becoming extratropical, (c) intensity, (d) location of storm circulation center relative to the coastline, (e) vertical wind shear, and f) time after landfall.

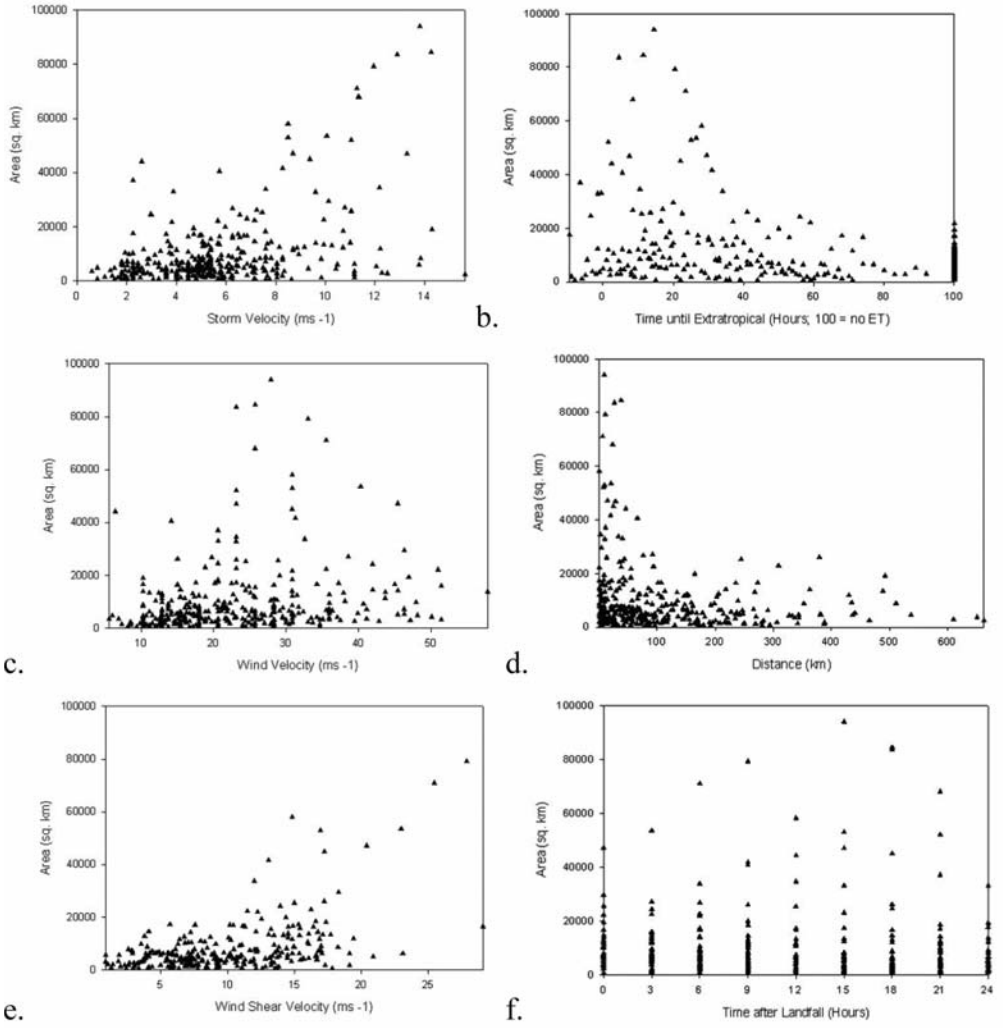

convection on average than do TCs experiencing less shear (Table 3, Figure 5e). Nine of the ten largest convective areas for highly-sheared TCs are associated with Floyd (1999) and Bertha (1996) when these TCs were approximately 20-35 hours from becoming extratropical and were located within 50 km of the coastline. Vertical wind shear typically increases during an extratropical transition (Jones et al., 2003), and moisture advection from the nearby ocean also contributes to the large area of rainfall associated with these highly-sheared TCs. However, strong vertical wind shear is not solely associated with an extratropical transition, as nearly 40% of the observations for highly-sheared storms occur in TCs that do not become extratropical within 72 hours of landfall. Many of these highly-sheared TCs that do not become extratropical have relatively small areas of convection surrounding their circulation centers as they track inland. Thus, a significant relationship does not exist between the speed of vertical wind shear and the area covered by convection (Table 1).

A negative correlation between the areal extent of convection and the time elapsed since landfall indicates that convection decreases in area over time (Table 1). The two highest averaged areas of convection occur at 12 and 18 hours post-landfall (Figure 5f), rather than at the time of landfall, which has the second smallest average area of convection (Table 3). At the time of landfall, convection tends to be organized into smaller regions in the eyewalls of hurricanes and/or the outer rainbands of hurricanes and weaker TCs. It is the dynamics associated with an extratropical transition that organizes these small regions of convection into larger regions and expands the overall size of the rain fields of the TCs. However, the overall size of the convective areas tends to decrease beginning approximately 12 hours prior to the TC becoming fully extratropical (Figure 5b), and this marked decrease in convection likely accounts for the negative correlation between the areal extent of convection and time elapsed since landfall.

CONCLUSION

A GIS was utilized to perform a spatial analysis of radar reflectivity returns to determine where regions of convective rainfall are located relative to the circulation centers of TCs, and how large an area was covered by these regions. The analysis was performed for 3-hourly periods during the first 24 hours after 43 TC landfalls. The radial and azimuthal positions of each convective region greater than 500 km^2 in area, and the total areal extent of convection at each observation time, were then examined relative to six factors. These factors were storm intensity, vertical wind shear, storm motion, whether the TC became extratropical, the number of hours elapsed since landfall, and the distance of the convective areas as well as the circulation center of the TC from the coastline.

This study supports the results of previous modeling and observational studies that suggest convection shifts counterclockwise and spreads outwards from the circulation center of TCs after landfall. Three factors are associated with a counterclockwise shift in convection from the right side to the front of the storm: a) increasing forward velocity, b) decreasing time until extratropical transition, and c) convection forming inland rather than offshore. However, increasing vertical wind shear shifts convection in the clockwise direction. The spreading outwards of convection is associated with a) decreasing storm intensity, b) increasing storm forward velocity, and c) decreasing time until a TC becomes extratropical.

Among the six factors examined in the current study, the forward velocity of the TC in conjunction with an extratropical transition had the strongest association with the location of convection both in the radial and azimuthal directions relative to the circulation center of the storm, and also the largest influence on the area over which convection extends. As the forward velocity of TCs increases due to interaction with a middle latitude trough, areas of convection grow in size, are located farther from the circulation center of the storm, and shift counterclockwise from the right side of

the storm when motion is slow to the front of the storm when motion is fast. The dynamical changes in the structure of a TC experiencing an extratropical transition act to decrease convection behind and in the core of the storm while increasing convection ahead of the storm so that the same pattern of shifting and growing convection is observed whether examining TCs according to their forward velocity or the time until they become extratropical.

Previous studies suggested that vertical wind shear is the dominant influence on the location of convection within TCs, but the current study found that shear did not have as strong of an association with the location of and area covered by convection as did storm motion and extratropical transition. As found by previous researchers, a clear maximum of convection in the downshear left quadrant convection was observed in the current study. However, a clockwise shift in the region where convection formed from upshear left to downshear right was observed as the velocity of the shear increased, which is a pattern that has not been discussed by previous researchers. Although the areas of convection were larger on average when TCs experienced high shear rather than shear with a velocity less than 10 m s^{-1}, the speed of the vertical wind shear did not significantly alter the radial position of the convection. These results suggest that the tendency to base the forecasted location of convective rainfall primarily on the direction and speed of the vertical wind shear may need to be reassessed.

This study analyzes a large number of TCs in a GIS framework. To more accurately determine specific locations on the ground that may experience convective rainfall from a TC, and to more effectively link the location of convective rainfall to environmental variables, future work should also utilize the GIS to quantify the shape and orientation of the convective regions. Adding these spatial attributes to the size and location data presented in the current study will allow a complete set of spatial attributes to be cataloged for each convective region. Analyzing these shapes at hourly or half-hourly intervals would facilitate the tracking of each convective region as it develops so that changes in its spatial attributes can be calculated as the TC tracks inland. Additional factors that may affect the development and displacement of convection such as the angle at which a TC crosses the coastline, topography, and moisture present within the atmosphere and soil, will also be considered so that these observational results can be compared to modeling studies that examine similar variables. The results of these future analyses could then be utilized to validate the spatial representation of convective rainfall regions produced by dynamical models such as the HWRF (Davis et al., 2008) and GFDL (Marchok et al., 2007), and statistical predictions of TC rainfall produced by models such as R-CLIPER (Marchok et al., 2007), TRaP (Kidder et al., 2005), and PHRaM (Lonfat et al., 2007).

Future research should also consider the contribution of stratiform rainfall to the total rainfall produced by TCs as they move over land. As convection diminishes, stratiform rainfall should comprise a larger portion of the rain fields as the TC moves inland. The techniques utilized in the current study should be applied to radar reflectivity regions having reflectivity values less than 40 dB*Z* to quantify the position and areal coverage of stratiform rainfall within the TC rain fields. The relative contribution of both stratiform and convective rainfall to the overall areal coverage of TC rain fields could then be calculated.

ACKNOWLEDGMENT

Three anonymous reviewers are thanked for their helpful comments that improved the quality of this manuscript.

REFERENCES

AMS. (2007). Hurricane forecasting in the United States. *Bulletin of the American Meteorological Society*, *88*, 87–92.

Anagnostou, E. N. (2004). A convective/stratiform precipitation classification algorithm for volume scanning weather radar observations. *Meteorological Applications*, *11*, 291–300. doi:10.1017/S1350482704001409

Atallah, E. H., & Bosart, L. R. (2003). The extratropical transition and precipitation distribution of Hurricane Floyd (1999). *Monthly Weather Review*, *131*, 1063–1081. doi:10.1175/1520-0493(2003)131<1063:TETAPD>2.0.CO;2

Bluestein, H. B., & Hazen, D. S. (1989). Doppler-radar analysis of a tropical cyclone over land - Hurricane Alicia (1983) in Oklahoma. *Monthly Weather Review*, *117*, 2594–2611. doi:10.1175/1520-0493(1989)117<2594:DRAOAT>2.0.CO;2

Burpee, R. W., & Black, M. L. (1989). Temporal and spatial variations of rainfall near the centers of two tropical cyclones. *Monthly Weather Review*, *117*, 2204–2218. doi:10.1175/1520-0493(1989)117<2204:TASVOR>2.0.CO;2

Cecil, D. J. (2007). Satellite-derived rain rates in vertically sheared tropical cyclones. *Geophysical Research Letters*, *34*2), L02811-L02821.

Chen, S. Y. S., Knaff, J. A., & Marks, F. D. (2006). Effects of vertical wind shear and storm motion on tropical cyclone rainfall asymmetries deduced from TRMM. *Monthly Weather Review*, *134*, 3190–3208. doi:10.1175/MWR3245.1

Corbosiero, K. L., & Molinari, J. (2002). The effects of vertical wind shear on the distribution of convection in tropical cyclones. *Monthly Weather Review*, *130*, 2110–2123. doi:10.1175/1520-0493(2002)130<2110:TEOVWS>2.0.CO;2

Corbosiero, K. L., & Molinari, J. (2003). The relationship between storm motion, vertical wind shear, and convective asymmetries in tropical cyclones. *Journal of the Atmospheric Sciences*, *60*, 366–376. doi:10.1175/1520-0469(2003)060<0366:TRBSMV>2.0.CO;2

Cubukcu, N., Pfeffer, R. L., & Dietrich, D. E. (2000). Simulation of the effects of bathymetry and land-sea contrasts on hurricane development using a coupled ocean-atmosphere model. *Journal of the Atmospheric Sciences*, *57*, 481–492. doi:10.1175/1520-0469(2000)057<0481:SOTEOB>2.0.CO;2

Davis, C., Wang, W., Chen, S. S., Chen, Y. S., Corbosiero, K., & DeMaria, M. (2008). Prediction of landfalling hurricanes with the Advanced Hurricane WRF model. *Monthly Weather Review*, *136*, 1990–2005. doi:10.1175/2007MWR2085.1

DeMaria, M., & Kaplan, J. (1994). A statistical hurricane intensity prediction scheme (SHIPS) for the Atlantic basin. *Weather and Forecasting*, *9*, 209–220. doi:10.1175/1520-0434(1994)009<0209:ASHIPS>2.0.CO;2

DeMaria, M., Mainelli, M., Shay, L. K., Knaff, J. A., & Kaplan, J. (2005). Further improvements to the statistical hurricane intensity prediction scheme (SHIPS). *Weather and Forecasting*, *20*, 531–543. doi:10.1175/WAF862.1

Elsberry, R. L. (2002). Predicting hurricane landfall precipitation: Optimistic and pessimistic views from the symposium on precipitation extremes. *Bulletin of the American Meteorological Society*, *83*, 1333–1339.

Frank, W. M., & Ritchie, E. A. (1999). Effects of environmental flow upon tropical cyclone structure. *Monthly Weather Review*, *127*, 2044–2061. doi:10.1175/1520-0493(1999)127<2044:EOEFUT>2.0.CO;2

Geerts, B., Heymsfield, G. M., Tian, L., Halverson, J. B., Guillory, A., & Mejia, M. I. (2000). Hurricane Georges's landfall in the Dominican Republic: Detailed airborne Doppler radar imagery. *Bulletin of the American Meteorological Society*, *81*, 999–1018. doi:10.1175/1520-0477(2000)081<0999:HGLITD>2.3.CO;2

Hill, K., & Lackmann, G. M. (2009). Influence of environmental humidity on tropical cyclone size. *Monthly Weather Review*, *137*, 3294–3315. doi:10.1175/2009MWR2679.1

Jones, R. W. (1987). A simulation of hurricane landfall with a numerical-model featuring latent heating by the resolvable scales. *Monthly Weather Review*, *115*, 2279–2297. doi:10.1175/1520-0493(1987)115<2279:ASOHLW>2.0.CO;2

Jones, S. C., Harr, P. A., Abraham, J., Bosart, L. F., Bowyer, P. J., & Evans, J. L. (2003). The extratropical transition of tropical cyclones: Forecast challenges, current understanding, and future directions. *Weather and Forecasting*, *18*, 1052–1092. doi:10.1175/1520-0434(2003)018<1052:TETOTC>2.0.CO;2

Jorgensen, D. P. (1984). Mesoscale and convective-scale characteristics of mature hurricanes. Part I: General observations by research aircraft. *Journal of the Atmospheric Sciences*, *41*, 1268–1285. doi:10.1175/1520-0469(1984)041<1268:MACSCO>2.0.CO;2

Kidder, S. Q., Kusselson, S. J., Knaff, J. A., Ferraro, R. R., Kuligowski, R. J., & Turk, M. (2005). The tropical rainfall potential (TRaP) technique. Part I: Description and examples. *Weather and Forecasting*, *20*, 456–464. doi:10.1175/WAF860.1

Kimball, S. K. (2008). Structure and evolution of rainfall in numerically simulated landfalling hurricanes. *Monthly Weather Review*, *136*, 3822–3847. doi:10.1175/2008MWR2304.1

Konrad, C. E., Meaux, M. F., & Meaux, D. A. (2002). Relationships between tropical cyclone attributes and precipitation totals: Considerations of scale. *International Journal of Climatology*, *22*, 237–247. doi:10.1002/joc.721

Lawrence, M. B., Avila, L. A., Beven, J. L., Franklin, J. L., Guiney, J. L., & Pasch, R. J. (2001). Atlantic hurricane season of 1999. *Monthly Weather Review*, *129*, 3057–3084. doi:10.1175/1520-0493(2001)129<3057:AHSO>2.0.CO;2

Lonfat, M., Marks, F. D., & Chen, S. Y. S. (2004). Precipitation distribution in tropical cyclones using the Tropical Rainfall Measuring Mission (TRMM) Microwave Imager: A global perspective. *Monthly Weather Review*, *132*, 1645–1660. doi:10.1175/1520-0493(2004)132<1645:PDITCU>2.0.CO;2

Lonfat, M., Rogers, R., Marchok, T., & Marks, F. D. (2007). A parametric model for predicting hurricane rainfall. *Monthly Weather Review*, *135*, 3086–3097. doi:10.1175/MWR3433.1

Marchok, T., Rogers, R., & Tuleya, R. (2007). Validation schemes for tropical cyclone quantitative precipitation forecasts: evaluation of operational models for US Landfalling cases. *Weather and Forecasting*, *22*, 726–746. doi:10.1175/WAF1024.1

Matyas, C. J. (2008). Shape measures of rain shields as indicators of changing environmental conditions in a landfalling tropical storm. *Meteorological Applications*, *15*, 259–271. doi:10.1002/met.70

Medlin, J. M., Kimball, S. K., & Blackwell, K. G. (2007). Radar and rain gauge analysis of the extreme rainfall during Hurricane Danny's (1997) landfall. *Monthly Weather Review*, *135*, 1869–1888. doi:10.1175/MWR3368.1

Molinari, J., Moore, P., & Idone, V. (1999). Convective structure of hurricanes as revealed by lightning locations. *Monthly Weather Review*, *127*, 520–534. doi:10.1175/1520-0493(1999)127<0520:CSOHAR>2.0.CO;2

Office of the Federal Coordinator of Meteorology. (2006). Federal Meteorological Handbook, No. 11: Doppler Radar Meteorological Observations- Part C: WSR-88D Products and Algorithms. *Washington, DC: U.S. Department of Commerce/ National Oceanic and Atmospheric Administration.*

Parrish, J. R., Burpee, R. W., Marks, F. D., & Grebe, R. (1982). Rainfall patterns observed by digitized radar during the landfall of Hurricane Frederic (1979). *Monthly Weather Review*, *110*, 1933–1944. doi:10.1175/1520-0493(1982)110<1933:RPOBDR>2.0.CO;2

Powell, M. D. (1990). Boundary-layer structure and dynamics in outer hurricane rainbands. 1. Mesoscale rainfall and kinematic structure. *Monthly Weather Review*, *118*, 891–917. doi:10.1175/1520-0493(1990)118<0891:BLSADI>2.0.CO;2

Rappaport, E. N. (2000). Loss of life in the United States associated with recent Atlantic tropical cyclones. *Bulletin of the American Meteorological Society*, *81*, 2065–2073. doi:10.1175/1520-0477(2000)081<2065:LOLITU>2.3.CO;2

Rodgers, E. B., Baik, J. J., & Pierce, H. F. (1994). The environmental influence on tropical cyclone precipitation. *Journal of Applied Meteorology*, *33*, 573–593. doi:10.1175/1520-0450(1994)033<0573:TEIOTC>2.0.CO;2

Rosenfeld, D., Wolff, D. B., & Atlas, D. (1993). General probability-matched relations between radar reflectivity and rain rate. *Journal of Applied Meteorology*, *32*, 50–72. doi:10.1175/1520-0450(1993)032<0050:GPMRBR>2.0.CO;2

Schwarz, F. K. (1970). Unprecedented rains in Virginia associated with remnants of Hurricane Camille. *Monthly Weather Review*, *98*, 851–859. doi:10.1175/1520-0493(1970)098<0851:TURIVA>2.3.CO;2

Shapiro, L. J. (1983). The asymmetric boundary-layer flow under a translating hurricane. *Journal of the Atmospheric Sciences*, *40*, 1984–1998. doi:10.1175/1520-0469(1983)040<1984:TABLFU>2.0.CO;2

Shepherd, J. M., Grundstein, A., & Mote, T. L. (2007). Quantifying the contribution of tropical cyclones to extreme rainfall along the coastal southeastern United States. *Geophysical Research Letters*, *34*, L23810. doi:10.1029/2007GL031694

Tuleya, R. E. (1994). Tropical storm development and decay: Sensitivity to surface boundary-conditions. *Monthly Weather Review*, *122*, 291–304. doi:10.1175/1520-0493(1994)122<0291:TSDADS>2.0.CO;2

Wilks, D. S. (1995). Statistical methods in the atmospheric sciences. San Diego, CA: Academic Press.

Willoughby, H. E., Marks, F. D., & Feinberg, R. J. (1984). Stationary and moving convective bands in hurricanes. *Journal of the Atmospheric Sciences*, *41*, 3189–3211. doi:10.1175/1520-0469(1984)041<3189:SAMCBI>2.0.CO;2

Corene Matyas is an assistant professor in the Department of Geography at the University of Florida, Gainesville, FL 32611-7315. Email: matyas@ufl.edu. Her research interests include tropical climatology with a focus on tropical cyclones and precipitation, and the GIS analysis of climate data and severe weather events.